34th Annual International Conference of the IEEE EMBS
San Diego, California USA, 28 August - 1 September, 2012

Study of Cardiac Pacemaker Excitation using Generic Ionic Models and Realistic Cell Distribution

Adrian D. Bradd, *Member, IEEE*, Amr Al Abed, *Member, IEEE*, Tianruo Guo, *Member, IEEE*, Nigel H. Lovell, *Fellow, IEEE*, Socrates Dokos, *Member, IEEE*

***Abstract*— Generic ionic models optimized to replicate experimentally recorded cardiac action potentials (APs) from the central and peripheral sinoatrial node (SAN), the natural pacemaker of the heart, as well as atrial intact-myocytes are implemented in a realistic 2D model of rabbit SAN geometry. The model was used to investigate two frequently-proposed modes of SAN architecture: the gradient and mosaic hypotheses. In a simplified gradient arrangement, the peripheral SAN region acts as a transition zone between the central SAN and atrium and is required for spontaneous rhythmic initiation of APs from central SAN into the atria. Furthermore, the application of optimized single cell parameters to the realistic 2D rabbit geometry did not accurately replicate experimentally recorded APs. On the other hand, in an adapted mosaic geometry, peripheral SAN cells were not required to produce spontaneous regular excitation.**

I. Introduction

Functional electrophysiology of the mammalian cardiac pacemaker, the sinoatrial node (SAN), is a topic of intensive research. Current electrophysiological methods, such as microelectrode recording and optical mapping, are unable to discern the time course of individual ionic currents from an action potential (AP) waveform. Historically, computer models have been used to investigate the dynamics of individual ionic currents. In general, there are two types of ionic models: biophysically-accurate ionic models and generic-phenomenological models, such as those utilized in the present study. Generic models, such as the FitzHugh Nagumo [1] and Fenton and Cherry [2], are computationally simpler than biophysically-accurate models which are time consuming to solve in 2D or 3D geometries [3]. Recently, a single cell generic ionic model for rabbit SAN and atria was published, optimized to match experimentally acquired APs [3]. The model characterizes central SAN (cSAN), peripheral SAN (pSAN) and right atrial myocytes using two Hodgkin Huxley [4] type active ionic currents and one background leakage current. This generic ionic model relies on the optimization of parameters and the selection of an appropriate number of voltage and time dependent ion currents to replicate APs. The use of higher order geometries, simplified or anatomically realistic, further increases the complexity and computation time of the models. Previously, it has been shown that the application of single cell models to higher order geometries is not a straight-forward process, often requiring the use of non-physiological values for parameters to produce stable and accurate APs [5]. In contrast, a number of studies have been published using simplified geometries with good results [6], [7], [8].

In the present study, generic ionic models of the SAN and atria [3] have been applied to a realistic 2D geometry of the rabbit cardiac pacemaker. Two geometrical models, simplified-gradient [9] and mosaic [10], are investigated. We analyze the importance of the transition zone in the simplified-gradient model, as well as describe the activation characteristics of the mosaic model.

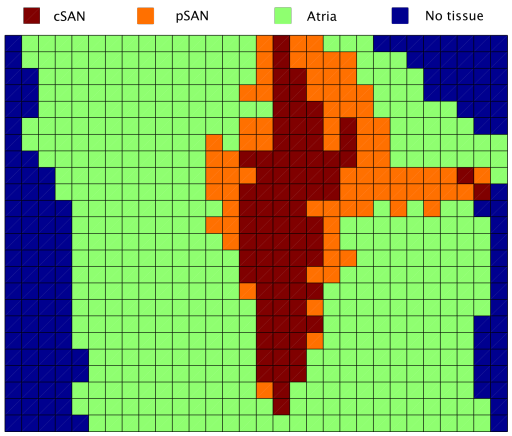

(a)

(b)

Figure. 1. Variations in cardiac pacemaker myocyte distribution from (a) the original Dobrzynski et al. [9] rabbit SAN data and (b) one of the five randomized mosaic cell geometries. The blue cells represent regions of no tissue; green represents atrial tissue, orange denotes pSAN and brown represents cSAN. The variation in pixelation is a direct result of the upscaling of the geometrical resolution for use in the mosaic simulations. Scale = 15 mm wide x 12 mm high.

Adrian Bradd, Tianruo Guo, Amr Al Abed, Nigel H. Lovell and Socrates Dokos are with the Graduate School of Biomedical Engineering, University of New South Wales, Sydney, 2052, Australia. (email: s.dokos@unsw.edu.au)

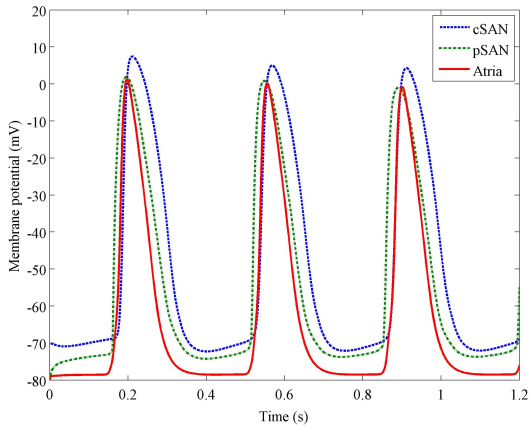

(a)

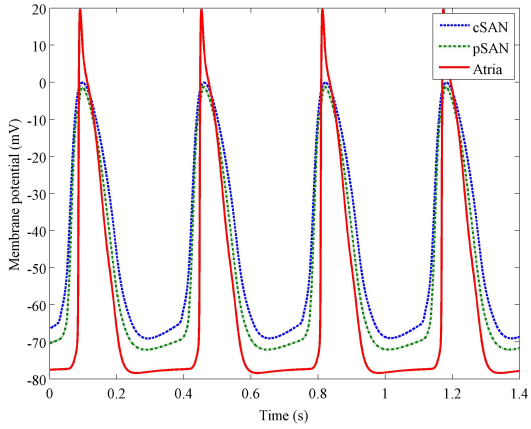

(b)

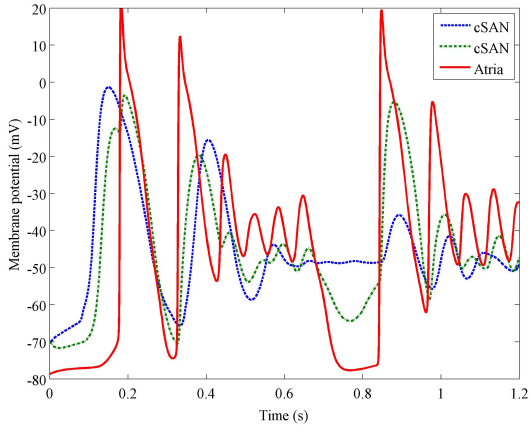

(c)

Figure. 2. (a) Parameters obtained by optimizing individual cSAN, pSAN and atrial single cell models. Notice here that the pSAN is leading the cSAN; Action potentials recorded from fixed points (cSAN, pSAN and atria) using various ionic model parameters. (b) APs generated using cSAN, pSAN and atrial parameters optimized in a 1D-axisymmetric cSAN-pSAN-atrial disc model [11]; (c) uses ionic parameters from (b) but with an altered geometry: the pSAN was replaced with cSAN extended. It is evident that the electrical activity is now unstable. Note that there are now two markers for cSAN, as a result of the pSAN being replaced with cSAN extended.

II. Methods

The ionic equations for the generic model have been previously described [3], [11]. Single cell parameters in the generic model were optimized to fit APs recorded from intact cSAN, pSAN and atrial myocytes [3]. The parameters were optimized under the assumption that the recorded data was from a single cell. A 1D axisymmetric disc, to reflect electrotonic loading in the SAN, was optimized to fit experimentally recorded AP data under the assumption that the cells are connected in a conductive continuum [11]. For each myocyte type, the generic model implemented in this study uses three ionic currents: an inward, outward and leakage current, with the former two utilizing two gate Hodgkin-Huxley dynamics. A monodomain cable-type formulation was used to describe conduction within the tissue [12]. Conductivities were chosen to achieve physiologically comparable waveshapes and correct entrainment of the pSAN and atria by the cSAN. They were: cSAN, 500 $[\mu S/cm^2]$; pSAN, 400 $[\mu S/cm^2]$; atria, 10000 $[\mu S/cm^2]$. Fibre angle was not considered in the model. Instead, the conductivites were taken to be an average over a specific region.

A. SAN geometry

The Dobrzynski et al. [9] geometry is a 3D anatomical model of the rabbit SAN and right atria. In this study, it was adapted to a 2D representation (Fig. 1a) as follows. For each x,y location, each cell in the z direction was scanned. If, at any depth (z), a cSAN cell was found, that 2D pixel became a cSAN, followed, in priority, by pSAN and atrium. This geometry represents the simplified-gradient model. The model was implemented in COMSOL Multiphysics 4.2a (COMSOL Inc.) finite-element software, and a number of iterations were run to obtain preliminary tissue conductivities and to produce spontaneous rhythmic activity in the cSAN and entrainment of the pSAN and atria.

B. Mosaic geometry

The mosaic geometrical data was generated using Matlab (Mathworks Inc.) from the original Dobrzynski et al. [9] geometry. Using published data for cellular distribution [10] the geometry upscaled (four cells for every one) and randomized depending upon the region. The crista region was designated to have a probability of 63% atrial myocytes (left of Fig. 1b); septal region, 88% atrial myocytes; and SAN 41% atrial myocytes. The entire mosaic model consisted of only two cell types: a single atrial cell type and a single SAN cell type (Fig. 1b).

III. Results

A. Dobrzynski geometry

Solutions to the generic ionic model applied to the Dobryznski et al. [9] rabbit cardiac pacemaker geometry can be seen in Fig. 2, showing snapshots of membrane potential against time. Initially, the model was implemented with the ionic parameters from Guo et al. [3], however the results were not ideal and it was difficult to select appropriate conductances. Initiation of APs occurred in the pSAN, as

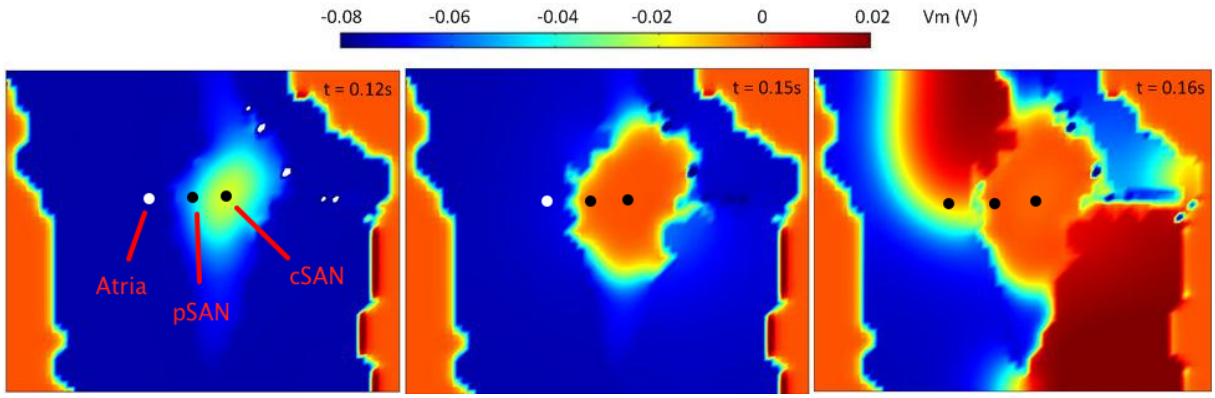

Figure. 3. Action potential propagation from cSAN to pSAN and into the atria. Time is increasing from left to right. The color bar along the top of the figure gives membrane potential (Vm). The three dots, labelled cSAN, pSAN and atria, correspond to the points at which membrane potential was recorded in Fig. 2

.

opposed to the cSAN, and the atrial action potential was rounded at the peak (Fig. 2a). Fig. 2b illustrates simulated APs using generic ionic models whose parameters have been previously optimized based on electrotonic loading in a simple disc SAN model [11]. In this case, it is evident that activation initiates in the cSAN and entrains the pSAN and the atria. In order to illustrate the stabilizing effect of the pSAN region, the pSAN was replaced with cSAN (Fig. 2c). The model was clearly unstable as a result of the absence of the pSAN, behaving arrhythmically. Fig. 3 illustrates the 2D spread of activation corresponding to the plots of Fig. 2b. Fig. 3 illustrates three snapshots of action potential propagation , with time increasing from left to right. As can be seen, activation originates from the center of the cSAN and propagates inferior and superior before activating the pSAN and then the atria.

B. Mosaic geometries

Activation sequences corresponding to the five random mosaic cell configurations are plotted in Fig. 4. It is evident that the point of initiation varies between each configuration. Furthermore, several configurations had multiple sites of activation (not shown). In every case, spontaneous rhythmic activation commenced in regions with high cSAN concentration and propagated into the surrounding atrial tissue. cSAN cell APs maintained their waveshape; however, atrial cell APs lost their sharp upstroke depolarization and repolarization, giving them a rounded appearance (not shown).

IV. Discussion

A. Dobrzynski geometry

cSAN, pSAN and atrial obtained from an axisymmetric 1D disc model [11] were assigned to the respective regions in the Dobrzynski et al. [9] rabbit SAN geometry. Results indicated spontaneous auto-rhythmic APs in which the cSAN fired first, subsequently activating the pSAN then the atria (Fig. 2b). Both the cSAN and pSAN displayed pacemaker potentials prior to activation, while the atria displayed stable resting potentials as expected. From the corresponding 2D activation time course in Fig. 3, initiation of the action potential began in the cSAN region, spreading through the pSAN and into the atria. The figure shows that conduction velocity is higher in the atria than the SAN: it takes 0.03s to activate the SAN but only 0.01s to activate the atria.

Using the same SAN, parameters optimized for a single cell cSAN, pSAN and atrial models [3] were also tested to illustrate the necessity for geometry specific optimization (Fig. 2a). The single cell-optimized parameters produced stable action potential waveforms, but initiation was in the pSAN, which subsequently entrained the cSAN and atria. The atrial waveform did not display a phase 1 early rapid repolarization (spike) as a result of inappropriate parameter values (Fig. 2a), which did not take into account the effect of electrotonic loading in the intact tissue. To test the hypothesis that the pSAN protects the cSAN from the hyperpolarizing effect of the atria, the pSAN was replaced with cSAN tissue in the original Dobrzynski geometry and membrane potentials were plotted in Fig. 2c. In this simulation, the atria did not suppress the cSAN; however, it is clear that the cSAN/atrial combination is unstable. A range of tissue conductivity values were tried in an attempt to attain stable cSAN firing and atrial activation, but without success. This result suggests that the pSAN may act as a stabilizer, protecting the cSAN from the hyperpolarizing load of the atria allowing the cSAN to rhythmically fire and activate the heart.

B. Mosaic geometries

Simulations were performed on five randomly-generated SAN mosaic geometries, consisting of only two cell-types: cSAN and atrial myocytes (Fig. 4). The results of these simulations indicated that the generic ionic model could be applied to a mosaic geometry and that there were significant shifts in the origin of pacemaker activation with fine differences in cell distribution. Often there were two sites of pacemaker activation, with one site suppressing the other upon activation of the atria (not shown). We noted that atrial cell APs were missing their characteristic rapid depolarization and repolarization, likely a result of a complex interaction between cSAN and atrial cells in close proximity.

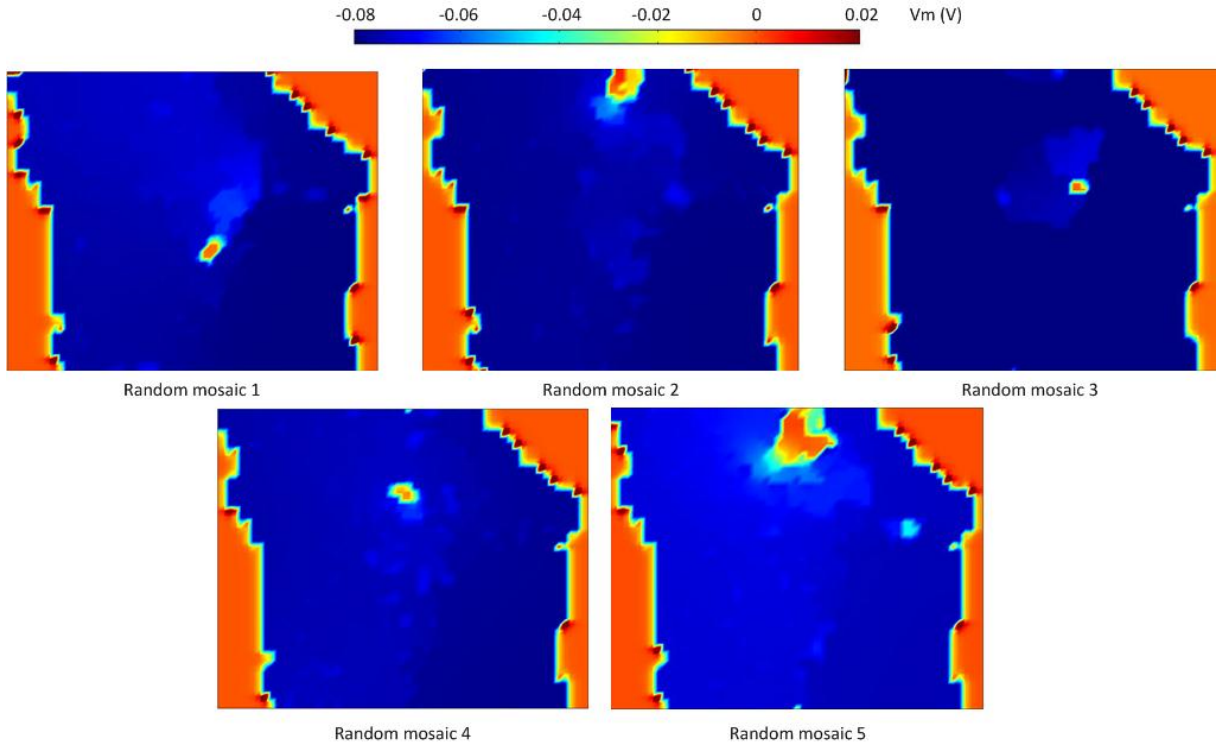

Figure. 4. Five random mosaic geometries were generated from published data [10]. Each model has a different initial point of activation (often there are two points of activation - not shown in all) suggesting that very slight changes in distribution can markedly alter activation of the SAN.

V. Conclusion

Generic ionic models were applied to a realistic 2D geometry of the mammalian cardiac pacemaker. The model parameters were chosen initially from a previous study on optimization of simplified atrial disc geometry. Resultant APs displayed good waveshapes, similar to those recorded experimentally using in-vitro rabbit sinoatrial tissue preparations, and initiation in the cSAN entrains both pSAN and atria. Application of optimized parameters obtained by fitting APs generated by single cell ionic models to experimental APs did not produce accurate waveshapes or a correct sequence of SAN entrainment, illustrating the need to optimize parameters for specific geometries. The pSAN, when removed from the model, led to unstable electrical activity, supporting the claim that the pSAN functionally protects the cSAN from the hyperpolarized atrial load. Mosaic models were also implemented by altering the 2D geometry such that atrial cells were interspersed through the SAN and vice versa. Results showed that the origin of pacemaker initiation is strongly dependent upon fine variances in SAN cell distribution. Future work is planned to optimize the model to fit APs from intracellular recordings of SAN and atrial cells as well as optical mapping of APs.

References

[1] J. M. Rogers and A. D. McCulloch, "A collocation-galerkin finite element model of cardiac action potential propagation," *Biomedical Engineering, IEEE Transactions on*, vol. 41, no. 8, pp. 743–757, Aug. 1994.

[2] A. Bueno-Orovio, E. M. Cherry, and F. H. Fenton, "Minimal model for human ventricular action potentials in tissue," *Journal of Theoretical Biology*, vol. 253, no. 3, pp. 544–560, 8 2008.

[3] T. Guo, A. A. Abed, N. H. Lovell, and S. Dokos, "A generic ionic model of cardiac action potentials," in *Engineering in Medicine and Biology Society (EMBC), 2010 Annual International Conference of the IEEE*. IEEE, 2010, pp. 1465–1468.

[4] A. Hodgkin and A. Huxley, "A quantitative description of membrane current and its application to conduction and excitation in nerve," *Bulletin of mathematical biology*, vol. 52, no. 1, pp. 25–71, 1990.

[5] A. Garny, P. Kohl, P. Hunter, M. Boyett, and D. Noble, "One-dimensional rabbit sinoatrial node models," *Journal of cardiovascular electrophysiology*, vol. 14, pp. S121–S132, 2003.

[6] S. L. Cloherty, S. Dokos, and N. H. Lovell, "A comparison of 1-D models of cardiac pacemaker heterogeneity," *Biomedical Engineering, IEEE Transactions on*, vol. 53, no. 2, pp. 164–177, 2006.

[7] R. Oren and C. Clancy, "Determinants of heterogeneity, excitation and conduction in the sinoatrial node: A model study," *PLoS Computational Biology*, vol. 6, no. 12, p. e1001041, 2010.

[8] H. Zhang, A. Holden, and M. Boyett, "Gradient model versus mosaic model of the sinoatrial node," *Circulation*, vol. 103, no. 4, pp. 584–588, 2001.

[9] H. Dobrzynski, J. Li, J. Tellez, I. Greener, V. Nikolski, S. Wright, S. Parson, S. Jones, M. Lancaster, M. Yamamoto, H. Honjo, Y. Takagishi, I. Kodama, I. Efimov, R. Billeter, and M. Boyett, "Computer three-dimensional reconstruction of the sinoatrial node," *Circulation*, vol. 111, no. 7, pp. 846–854, 2005.

[10] E. Verheijck, A. Wessels, A. van Ginneken, J. Bourier, M. Markman, J. Vermeulen, J. de Bakker, W. Lamers, T. Opthof, and L. Bouman, "Distribution of atrial and nodal cells within the rabbit sinoatrial node: models of sinoatrial transition," *Circulation*, vol. 97, no. 16, pp. 1623–1631, 1998.

[11] A. A. Abed, T. Guo, N. H. Lovell, and S. Dokos, "Tissue-based optimization of a sino-atrial node disc model," in *Engineering in Medicine and Biology Society, EMBC, 2011 Annual International Conference of the IEEE*. IEEE, 2011, pp. 1375–1378.

[12] J. Jack, D. Noble, and R. Tsien, *Electric current flow in excitable cells*. Clarendon Press Oxford, 1975.